Am J Physiol Gastrointest Liver Physiol 322: G142–G153, 2022.
First published December 1, 2021; doi:10.1152/ajpgi.00060.2021

american physiological society

AMERICAN JOURNAL OF PHYSIOLOGY
GASTROINTESTINAL AND LIVER PHYSIOLOGY

RESEARCH ARTICLE

NMDA receptor expression during cell transformation process at early stages of liver cancer in rodent models

Yurii V. Stepanov,[1] Iuliia Golovynska,[1] Nataliia V. Dziubenko,[2] Halyna M. Kuznietsova,[2] Nataliia Petriv,[3] Inessa Skrypkina,[4] Sergii Golovynskyi,[1] Liudmyla I. Stepanova,[3] Yevhenii Stohnii,[3] Liudmyla V. Garmanchuk,[3] Liudmyla I. Ostapchenko,[3] Tetyana Yevsa,[3] Junle Qu,[1] and Tymish Y. Ohulchanskyy[1]

[1]*Center for Biomedical Optics and Photonics, College of Physics and Optoelectronic Engineering, Shenzhen University, Shenzhen, People's Republic of China;* [2]*Institute of Biology and Medicine, Taras Shevchenko National University of Kyiv, Kyiv, Ukraine;* [3]*Department of Gastroenterology, Hepatology and Endocrinology, Hannover Medical School, Hannover, Germany; and* [4]*Institute of Molecular Biology and Genetics, National Academy of Sciences of Ukraine, Kyiv, Ukraine*

Abstract

Hepatocellular carcinoma (HCC) is the most common primary liver cancer, which is not sensitive to radiotherapy and chemotherapy and very often experiences postoperative relapse. In this regard, effective screening of liver cancer is considered as the most important and urgent task. The aim of our study was to determine whether *N*-methyl-D-aspartate receptor (NMDAR) and, in particular, its subunits, can serve as biomarkers to distinguish the precancerous liver at early stages of liver fibrosis. We assessed the development of HCC after 10, 15, and 22 wk using a HCC rat model. The expression of NMDAR subunits was monitored at different stages of HCC by means of immunohistochemistry combined with epifluorescence microscopy imaging, Western blotting, and direct bisulfite sequencing. NMDAR subunits were not found in healthy liver tissues. In contrast, NMDAR subunits, in particular NR1 and NR2B, appeared at the stage of severe liver fibrosis (precancerous liver disease) in rats and were expressed during the development of HCC in rats and mice. Using the direct bisulfite sequencing, we detected that increased expression of NMDAR directly correlated with the demethylation of CpG islands in the promoter region of genes encoding receptor subunits. The obtained results confirmed that NMDAR subunits can serve as new biomarkers of precancerous liver disease, severe fibrosis, and its progression towards HCC.

NEW & NOTEWORTHY We have shown NMDAR expression in cell transformation process at early stages of cancer, specifically HCC. The aim of our study was to define the disease stages from precancerous liver disease towards liver cancer progression when NMDAR subunits were expressed/detected. A fibrosis/HCC rat model, immunohistochemistry combined with epifluorescence microscopy imaging, Western blotting was used. The dynamics of appearance of NMDAR subunits, their expression and methylation status during the development of HCC were shown and discussed.

hepatocellular carcinoma; liver fibrosis; N-methyl-D-aspartate receptor; NMDAR subunit; precancerous conditions

INTRODUCTION

Liver cancer or hepatocellular carcinoma (HCC) is a malignant tumor that occurs in the hepatic lobes and represents the third deadliest cancer worldwide with 830,000 deaths annually (https://www.who.int/news-room/fact-sheets/detail/cancer). The disease is characterized by a rapid tumor growth and is difficult to treat. HCC can be instigated by the hepatitis viruses, alcohol, nonalcoholic steatohepatitis, or as a result of infection-caused chronic inflammation (1), or also as a result of action of various types of toxins (e.g., mold aflatoxins) (2). Symptoms of the earliest stage of liver cancer are very weak; patients can only feel fatigue and weakness. Most patients cannot get timely treatment due to a late diagnosis, undergoing surgical removal or liver transplantation; the survival rate of patients with HCC is low with a high recurrence rate after surgery (3, 4). Therefore, early detection of HCC, especially at the precancerous stage, is necessary for effective and timely treatment and improvement of long-term survival.

Recently, glutamate receptors (GluRs), in particular, such as *N*-methyl-D-aspartate receptor (NMDAR), have drawn an increasing interest as regulators of carcinogenesis and possible precancerous markers (5, 6). NMDAR has seven subunits: NR1, NR2A/B/C/D, NR3A/B, each one is encoded by a separate gene; alternative splicing results in complementary heterogeneity of NMDAR subunits. NMDAR is a tetramer that comprises two obligatory NR1 subunits and two regulatory subunits, like NR2A/B/C/D, which bond together to form a dimer (7). The forming complex might eventually connect with either NR3A or NR3B, which can replace one of four NR2 subunits (6, 7). In NMDAR, NR1 subunit is required for calcium conductivity of the channel, whereas NR2 and NR3 subunits

Correspondence: T. Y. Ohulchanskyy (tyo@szu.edu.cn); L. V. Garmanchuk, (liudmyla_garmanchuk@ukr.net).
Submitted 15 February 2021 / Revised 10 November 2021 / Accepted 27 November 2021

define pharmacological and electrophysiological properties of the receptor. Because of the variety of NMDAR subunits, the receptors with special physicochemical and pharmacological properties can be formed (8). Besides the central nervous system (9), the presence of NMDARs has been found in peripheral cells (10–14).

Importantly, NMDAR subunits were demonstrated to be expressed in all investigated cancer cell lines and tumors, even if they are absent in healthy tissue of the same organ. NR1 subunit of NMDAR is known to be overexpressed in colorectal (15) and prostate cancer (16); in contrast, its expression is known to be low in normal tissues. Different combinations or single subunits of NMDARs were established in cell lines derived from cells melanoma (17), osteosarcoma (18), gastric cancer (19), oral squamous cell carcinoma (20), leukemia and lymphoma (21), thyroid cancer (22), lung cancers (23), breast cancer (24), pancreatic (25), laryngeal carcinoma (26), hepatocellular (27), and ovarian cancer (28). A number of studies have shown that NMDARs are functionally active in cancer cells: they are necessary for cancer cell survival and proliferation, and their blockade reduced cell active growth and viability (22, 29–31). In particular, NMDAR expression and activation result in restraining apoptosis by blocking forkhead box O; they also lead to an increase in mammalian target of rapamycin signaling activity, which serves as a connecting link between NMDAR and cancer (31, 32).

As a reason, causing a change in the expression of NMDARs during carcinogenesis may be either somatic mutations in genes, encoding the NMDAR subunits (33, 34), or epigenic changes, associated with the methylation status of the CpG islands of NMDAR subunits. Aberrant methylation status of NR2B promoter has been found in gastric cancer (35), in non-small cell lung cancer (NSCLC) (10), and at the breast cancer progression (36). Literature data have shown that methylation of NR2B gene has an inverse correlation with gene expression (10, 37), as well as NR2B methylation was related with better prognosis and survival in patients with NSCLC (10).

Based on the foregoing, it can be summarized that the altered receptor expression is associated with any neoplastic process ongoing and contributes to cancer progression. Since NMDAR expression is a widespread event that accompanies neoplastic transformation of cells, the appearance of these receptors can serve as an early marker of cancer.

To the best of our knowledge, currently there are no reports that show NMDAR expression in cell transformation process at early stages of cancer, specifically HCC. Therefore, the aim of our study was to define the disease stages from precancerous liver disease toward liver cancer progression when NMDAR subunits were expressed and/or detected. The expression of NMDAR subunits, using a fibrosis/HCC rat model and murine models of liver fibrosis and HCC, was monitored by means of immunohistochemistry combined with epifluorescence microscopy imaging and Western blotting. The dynamics of appearance of NMDAR subunits, their expression, and methylation status during the development of HCC were shown and discussed.

MATERIALS AND METHODS

Animals

The animal studies were carried out at the Taras Shevchenko National University of Kyiv, Ukraine, using healthy Wistar male rats, 4 mo old, weighing 180–200 g, in strict accordance with the Law of Ukraine of 21.02.2006 No. 3447-IV "On protection of animals from cruel treatment," the recommendations by the National Institutes of Health about the general ethical principles of animal experiments described in *Guide for the Care and Use of Laboratory Animals* (National Academy Press, Washington D.C.: 1996) and the experimental protocols approved by the Bioethics Committee for Animal Experiments in the Institute of Biology and Medicine at the Taras Shevchenko National University of Kyiv, Ukraine (Animal Experiment Application Approval No. 2 of February 7, 2020). Before the experiments, rats were maintained in collective cages under standard controlled conditions on a 12-h light/dark cycle and fed standard rodent chow and water ad libitum.

Mice samples were prepared at the Hannover Medical School in accordance to institutional guidelines and in compliance with ethical regulations and the approval of the LAVES (AZ 18/2808, 20/3419). Mice were maintained under specific pathogen-free conditions on standard rodent diet and water which were provided to the animals ad libitum.

Model of Liver Fibrosis and Carcinogenesis in Rats and Mice

To initiate liver fibrosis and subsequently hepatic carcinogenesis in rats, the chemical hepatocarcinogen *N*-diethylnitrosamine (DEN) was dissolved in physiological saline and intraperitoneally injected in a single dose (200 mg/kg). Control animals were intraperitoneally injected only physiological saline. After 2 wk, hepatotoxin (also known as tetrachloromethane CCl_4, carbon tetrachloride, Freon-10), diluted in sunflower oil at a ratio of 1:1, was subcutaneously injected twice a week for 20 wk, in the amount of 0.1 mL/100 g of rat body weight to stimulate more intensive tumor development (38). Control animals were subcutaneously injected with only sunflower oil. The detailed scheme of hepatic carcinogenesis is described in the Supplemental Material (all Supplemental Material is available at https://doi.org/10.6084/m9.figshare.14014946).

In experimental animals, the liver observations were performed after 10, 15, and 22 wk since the beginning of oral CCl_4 injection in comparison to the control healthy livers. The animals of inspected groups (n = 10 per group) were randomly allocated in numbered collective cages, before the experiment start.

To induce liver fibrosis in mice, wild-type C57BL/6J mice were treated as previously described (39, 40). Briefly, 6-wk-old C57BL/6J mice were treated with 4 μL/g body wt. of 10% CCl_4 solution diluted in sunflower oil for 8 wk (intraperitoneal administration twice per week). Control mice were administered with NaCl or sunflower oil (4 μL/g body wt.).

HCC in mice was induced, using a transposon-mediated stable intrahepatic transfer of oncogenic $NRAS^{G12V}$ in $p19^{Arf-/-}$ mice (41), as established in previous studies (42–44). Control mice were injected with the effector loop mutant $Nras^{G12V/D38A}$, which does not result in HCC development. DNA vectors [transposon and Sleeping Beauty 13 (SB13) transposase] were prepared using the QIAGEN EndoFree Maxi Kit (QIAGEN, Hilden, Germany). Transposon and transposase vectors were mixed in a 5:1 molar ratio and injected to mice, using hydrodynamic tail vein injection (HDI), as described previously (42–44).

Immunohistochemistry and Fluorescence Microscopy

Liver slices obtained upon sampling of rats were transferred into 35-mm glass-bottom microwell dishes and incubated with anti-NMDA-NR1 (RRID AB_2551951), NR2A (RRID AB_2735295), NR2B (RRID AB_2534001), NR2C (RRID AB_2607805), NR2D (RRID AB_2736237), and NR3A/NR3B (RRID AB_2232559) polyclonal antibodies (all used antibodies have green fluorescent, $\lambda_{excitation}$ = 490 nm/$\lambda_{emission}$ = 515 nm), according to the manufacturer's instructions (Thermo Fisher Scientific, China). Cells were probed for 24 h at 4°C in a humidified chamber with anti-NMDA-NR antibodies at 1 μg/mL diluted in 50 mM Tris·HCl, pH 7.4, containing 1.5% NaCl, 0.3% Triton X-100, and 4% normal goat serum. To prevent a nonspecific binding and background staining, before applying anti-NMDAR antibodies, cells were incubated with 0.3% Triton X-100 and 4% normal goat serum for 1 h following a standard method (30). All samples were inspected at the same parameters of epifluorescence imaging, employing a Nikon Eclipse Ti-U inverted microscope equipped with a camera (Nikon, Japan) at ×20magnification. The sample size and scale bar were determined using the Nikon Eclipse Ti-U microscope software NIS Elements. For quantitation of fluorescence intensity of NMDAR subunits, ImageJ software was used.

Bisulfite Sequencing

Genomic DNA was extracted from normal liver tissue of rats after 10, 15, and 22 wk of hepatic carcinogenesis development, using NucleoSpin Tissue Kit (MACHEREY-NAGEL, Düren, Germany), followed by conversion of bisulfite to 1 μg of genomic DNA, using the EpiTect Bisulfite Kit (Qiagen, Hilden, Germany), according to the manufacturer's protocols.

Bisulfite sequencing was performed analogously to the protocol described by R. Ryley Parrish (45, 46). Bisulfite-treated DNA was amplified using primers (Table 1) focused on the CpG islands of the Glutamate Ionotropic Receptor NMDA Type Subunit 1 (*GRIN1*) (2534156–2534805, Sequence ID: NC_005102.4), *GRIN2A* (5710495-5709910 bp, Sequence ID: NC_005109.4), (41) GRIN2B (169999124–169999329, Sequence ID: NC_005103.4) (46), and *GRIN2C* (10381636–103816968 bp, Sequence ID: NC_005109.4).

CpG islands in the promoter region of the *GRIN1* and *GRIN2C* rat genes were determined using the University of California, Santa Cruz (UCSC) Genome Browser (UCSC Genome Informatics Group, Santa Cruz, CA). Primers were selected using Methyl Primer Express Software v1.0 (Applied Biosystems, Foster City, CA). All primers were verified on rat DNA artificially methylated with CpG methyltransferase SssI (M.SssI) (Thermo Fisher Scientific).

Bisulfite-modified DNA (2 μL) was subjected to PCR amplification in a final reaction volume of 20 μl 1X HOT FIREPol Blend Master Mix Ready to Load (Solis BioDyne, Tartu, Estonia) and 0.5 μM of each primer. PCR was performed with an initial 15 min incubation at 95°C, followed by 40 cycles of denaturation at 95°C for 1 min, annealing at 60°C for 1 min, extension at 72°C for 1 min, and a final 7-min hold at 72°C and then terminated at 4°C. Detection of the gel images was performed using a ChemiDoc XRS+ System (Bio-Rad Laboratories, Inc., Hercules, CA). PCR fragments were purified using NucleoSpin Gel and PCR Clean-up (MACHEREY-NAGEL, Düren, Germany). Sequencing was performed with a forward primer using the Applied Biosystems 3130 Genetic Analyzer sequencer (Applied Biosystems, Life Technologies) with the BigDye Terminator v3.1 Cycle Sequencing Kit. Electrophoregram analyzed using SnapGene Viewer 5.1.5 software (GSL Biotech LLC, San Diego, CA). The percent methylation of CpG sites was determined by the ratio between the peak values of the height of cytosine (C) and thymine (T), giving the basic equation for the percentage of methylation (C/(C + T)·100), as described (45).

Schemes of CpG sites in the research regions were created using SnapGene Viewer 5.1.5 software (GSL Biotech LLC, San Diego, CA). Determination of the methylation sequence of CpG lanes by direct bisulfite sequencing began from the first methylated island in the promoter regions of genes. The methylation level analysis using forward primers comprised CpG sites starting from the 5'-end of CpG islands.

All other materials and methods are listed in the Supplemental Material.

RESULTS

Rat Model of Liver Fibrosis/HCC Development

Development of precancerous liver disease (fibrosis) and subsequently liver cancer (HCC) were initiated in rats using the inducer of malignant transformation DEN and hepatotoxin CCl_4. Over 22 wk after DEN injection, the development of liver disease was observed; during the first 2–6 wk, the liver inflammation was noted, then after 8–12 wk, the fibrosis and cirrhosis developed and followed by liver malignant transformation (detected at the 14th–16th wk), which progressed to advanced fibrosis/HCC, with visible multiple tumor nodes in all liver parts, till the 20th–22nd wk (Fig. 1*A*). Hence, it was decided to perform the liver observation and biochemical studies after 10, 15, and 22 wk, when the alterations of tissue structure were distinctly visible, in comparison to control healthy rats. The following study groups (n = 10) are described as: 0 wk, control; 10 wk, fibrosis/HCC development and cirrhosis; 15 wk, progressive cirrhosis and initiation of malignant transformation; and 22 wk, progressive HCC (Fig. 1, Supplemental Figs. S1 and S2).

After animal euthanasia and dissection, the liver macroscopic damage score was graded by the 13-point scale (38) (see supporting methods in the Supplemental Material); all control animals had a healthy liver, which correlated in the

Table 1. *Primers used for the DNA bisulfite sequencing analysis*

Primer ID	Primer Forward (5'–3')	Primer Reverse (5'–3')	Size, bp
GRIN1	TAGTTATTGAAGGTTTGGGAT	CGTTAAACTATATCTTCCAAAAAC	650
GRIN2A[41]	AGTGAGTGATAAAAGTAGTTAGTG	ATCTCTTCCTAACCTTACCTTAT	586
GRIN2B[40]	TTTTTTAGGGGAGAGGTTGAGTAGC	AATAAAACACACTAACACGCGCGTA	207
GRIN2C	CGTTTTAGGCGAAGGGAAGA	AACGACCGAAAATAACGAACTC	603

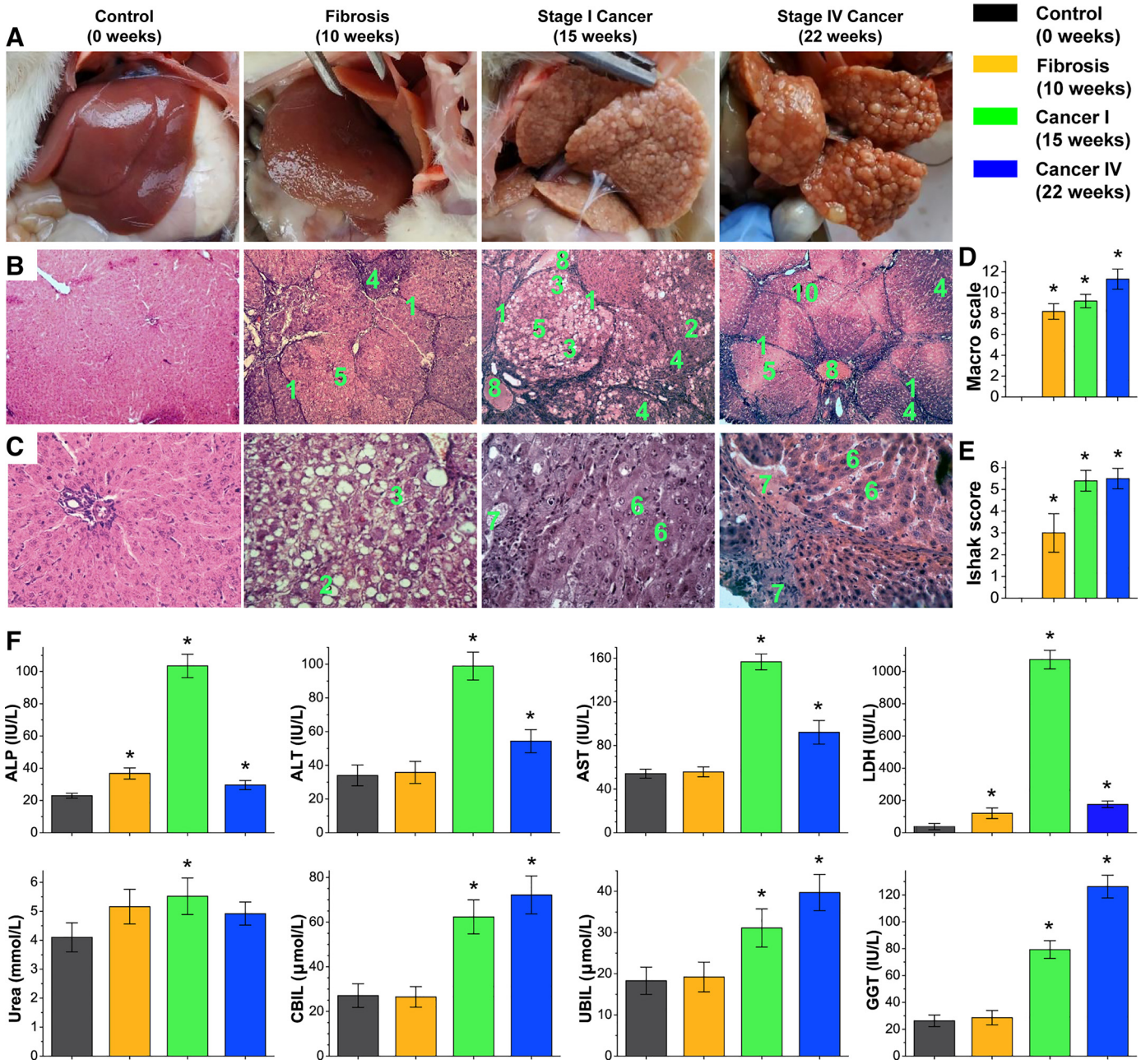

Figure 1. DEN/CCl_4 model of liver fibrosis progressing toward HCC in Wistar rats. *A*: whole liver during fibrosis/HCC development after 10, 15, and 22 wk of treatment in comparison to healthy rat liver as control. The representative slices of rat liver [hematoxylin and eosin staining, ×100 (*B*), ×400 (C)] during fibrosis/HCC development. Numbers are depicting: portal–portal linking septs (1), lipid (2), and balloon dystrophy (3), basophilic cell alteration (4), hepatocellular hypertrophy (5), ground-glass hepatocytes (6), necrotic cells (7), increase blood volume in vessels (8), oval cell hyperplasia (9), eosinophilic cell alteration (10). *D*: liver macroscopic damage level evaluated by the 13-point scale. *E*: fibrosis level evaluated using the Ishak score. *F*: levels of serum ALP, ALT, AST, LDH, urea, CBIL, UBIL, and GGT. The data are presented as the means ± SD ($n = 10$) with $^*P < 0.05$ compared with controls. Liver macroscopic (*B*) and microscopic damage (*C*) level evaluated by the 13-point scale. ALP, alkaline phosphatase; ALT, alanine aminotransferase; AST, aspartate aminotransferase; CBIL, conjugated bilirubin; GGT, gamma-glutamyl transferase; HCC, hepatocellular carcinoma; LDH, lactate dehydrogenase; UBIL, unconjugated bilirubin.

scale with 0 points (Fig. 1, *B–E* and Supplemental Fig. S2, *A* and *B*). At the stage of fibrosis after 10 wk, the degree of liver damage correlated with 8.2 ± 0.9 points (Fig. 1, *B* and *D* and Supplemental Fig. S2*C*). The activity of alkaline phosphatase (ALP) and lactate dehydrogenase (LDH) increased 1.6 and 3.2 times, respectively. Urea content in the blood serum also increased by 26%. However, alanine aminotransferase (ALT), aspartate aminotransferase (AST), γ-glutamyl transferase (GGT) activities, total protein, urea, and conjugated (CBIL) and unconjugated bilirubin (UBIL) concentrations were not changed in comparison with control groups (Fig. 1*F*). At the microscopic level, the accumulation of connective tissue was observed in the form of well-developed portal-portal linking septs, and hepatocytes' micro- and macrovesicular lipid

dystrophy, basophilic cell alteration, and hepatocellular hypertrophy were observed. Ground-glass hepatocytes, a sign of liver toxicity, were found in some places (Fig. 1*C* and Supplemental Fig. S2*D*). The fibrosis level on the Ishak score correlated with 3.0 ± 0.88 points (the Ishak score stages are described in supporting methods of the Supplemental Material) that corresponded to *stage I–II* liver fibrosis (Fig. 1*E*).

After 15 wk of fibrosis/HCC development, the liver damage progressed in all animals. At the macroscopic level, the degree of liver damage correlated with 9.2 ± 0.79 points (Fig. 1, *B* and *D*, and Supplemental Fig. S2*E*). The macronodular cirrhosis was indicated; 6 of 10 animals had tumor nodes (1 per animal). In blood serum, ALP and LDH increased sharply to 4.5 and 28.5 times, respectively, ALT and AST to 2.9 and 2.8 times, respectively, CBIL and UBIL to 2.3 and 1.7 times, respectively, and GGT to 3.2 times. Urea content in serum increased by 35% (Fig. 1*F*). At microscopic level, the development of cirrhosis was observed: thick septa of connective tissue with islets of liver parenchyma between them, lipid and balloon dystrophy of hepatocytes with necrotic cells, increased blood volume in vessels (which is a sign of portal hypertension, typical complication in cirrhosis), large amount of ground-glass hepatocytes, and hepatocellular hypertrophy were evident upon inspection (Fig. 1*C* and Supplemental Fig. S2*F*). The unchanged liver tissue was almost absent (Fig. 1*C*). The level of fibrosis at this time point correlated with 5.4 ± 0.48 points (Fig. 1*E*).

After 22 wk of HCC development, the degree of liver damage correlated with 11.3 ± 1.1 points, which corresponds to the stage IV cancer (Fig. 1*D*). The multiple nodes of different sizes were observed against the background of cirrhotic changes (Fig. 1, *B* and *C* and Supplemental Fig. S2*G* and *H*). In blood serum, ALP was increased to 1.2 times, GGT to 4.9 times, LDH to 4 times, ALT and AST to 1.3 and 1.7 times, respectively, and CBIL and UBIL to 2.7 and 2.17 times, respectively. Urea content in serum increased to 1.2 times (Fig. 1*F*). A thorough histopathological analysis performed by an experienced pathologist revealed that the cirrhosis developed in all animals after 22 wk (Fig. 1, *B* and *C* and Supplemental Fig. S2, *G* and *H*). In particular, the following changes were noted: *1*) significant deposits of connective tissue around portal areas, thick inter-portal connective septa and formed connective tissues nodes; *2*) liver parenchyma islets are represented by very large cells with light cytoplasm (hepatocellular hypertrophy) or cells with eosinophilic or basophilic alteration (preneoplastic changes, also can be adenoma); *3*) areas of ground-glass hepatocytes, areas of cells with micro- and macrovesicular lipid dystrophy, widespread necrosis, signs of portal hypertension (dilated blood vessels), and oval cell hyperplasia (intense regenerative processes) were observed. The representative hematoxylin and eosin (H&E) images are shown in Fig. 1, *B* and *C* and Supplemental Fig. S2, *G* and *H*. The level of liver damage at this stage on the Ishak score correlated with 5.4 ± 0.48 points (Fig. 1*E*).

NMDAR Subunits, in Particular, NR1, NR2B-D, Are Detected via Immunofluorescence in Fibrotic Livers

We first investigated the dynamics of NMDAR subunits formation in the liver in each study group of rats. The subunit formation was assessed through the immunohistochemistry staining of liver slices, using fluorescently labeled antibody targeting specifically different NMDAR subunits, which correlated with the number of receptors on cell membrane (Fig. 2 and Supplemental Fig. S3). The quantitation of fluorescence intensity of NMDAR subunits was performed using ImageJ software.

NMDAR subunits were not found in the liver slices collected from the control healthy animals (Supplemental Fig. S3*A*). At the fibrosis stage after 10 wk, the analysis showed the appearance of fluorescently labeled NMDAR subunits (Fig. 2 and Supplemental Fig. S3, *B–F*). Through accessing the composition of NMDAR subunits, the formation of four subunits [NR1 (gene *GRIN1*), NR2B (gene *GRIN2B*), NR2C (gene *GRIN2C*), and NR2D (gene *GRIN2D*)] was shown, where NR1 and NR2B manifested the most intense fluorescence signal (i.e., the highest expression). After 15 wk of fibrosis/HCC development, five subunits [NR1, NR2A (gene *GRIN2A*), NR2B, NR2C, and NR2D] were identified. It is notable that NR2A subunit expressed in the bile duct walls; NR1 and NR2B subunits displayed the most intense fluorescence signal. After 22 wk (stage of a full blown HCC), six subunits [NR1, NR2B, NR2C, NR2D, NR3A (gene *GRIN3A*), and NR3B (gene *GRIN3B*)] were detected. NR2A subunit was not found, though NR3A and NR3B were additionally formed at this stage, in comparison to the previous one. NR1 and NR2B subunits have shown the brightest fluorescence signal in this group also, whereas other subunits were less pronounced.

Western Blotting Analysis Revealed the Presence of NR1, NR2B-C NMDAR Subunits Already in Fibrotic Livers

We next performed the determination of NMDAR subunits in hepatocyte plasma membranes in each group of animals during the development of liver disease from fibrosis toward HCC using Western blotting. NMDAR subunits were not detected in control healthy group (Fig. 3). At the stage of fibrosis after 10 wk, four subunits (NR1, NR2B, NR2C, and NR2D) were determined in rat liver samples. The amount of NR2D was found to be minor. After 15 wk, five subunits (NR1, NR2A, NR2B, NR2C, and NR2D) were determined, where NR2A expression was the lowest. After 22 wk of HCC development, six subunits (NR1, NR2B, NR2C, NR2D, NR3A, and NR3B) were determined. So, NR2A subunit was not observed; however, NR3A and NR3B were weekly expressed. The highest expression was observed for NR1, NR2B, and NR2C subunits, whereas other subunits were less pronounced at all the stages of fibrosis/HCC development in rats.

We further tested the presence of NR1 in transposon-based HCC (genotype: $p19^{Arf-/-}/NRAS^{G12V}$) and CCl_4-induced liver fibrosis in mice. In line with our data shown in rats, murine HCC showed a high expression of NR1 subunit in comparison to control groups (Supplemental Fig. S4). Interestingly, we did not observe NR1 in fibrotic livers of mice, which were treated for 8 wk with CCl_4 and did not develop HCC (Supplemental Fig. S4). The latter confirmed that NR1 can be detected only in severe fibrosis, which develops toward HCC, as we have shown using CCl_4/DEN model in rats (Fig. 3).

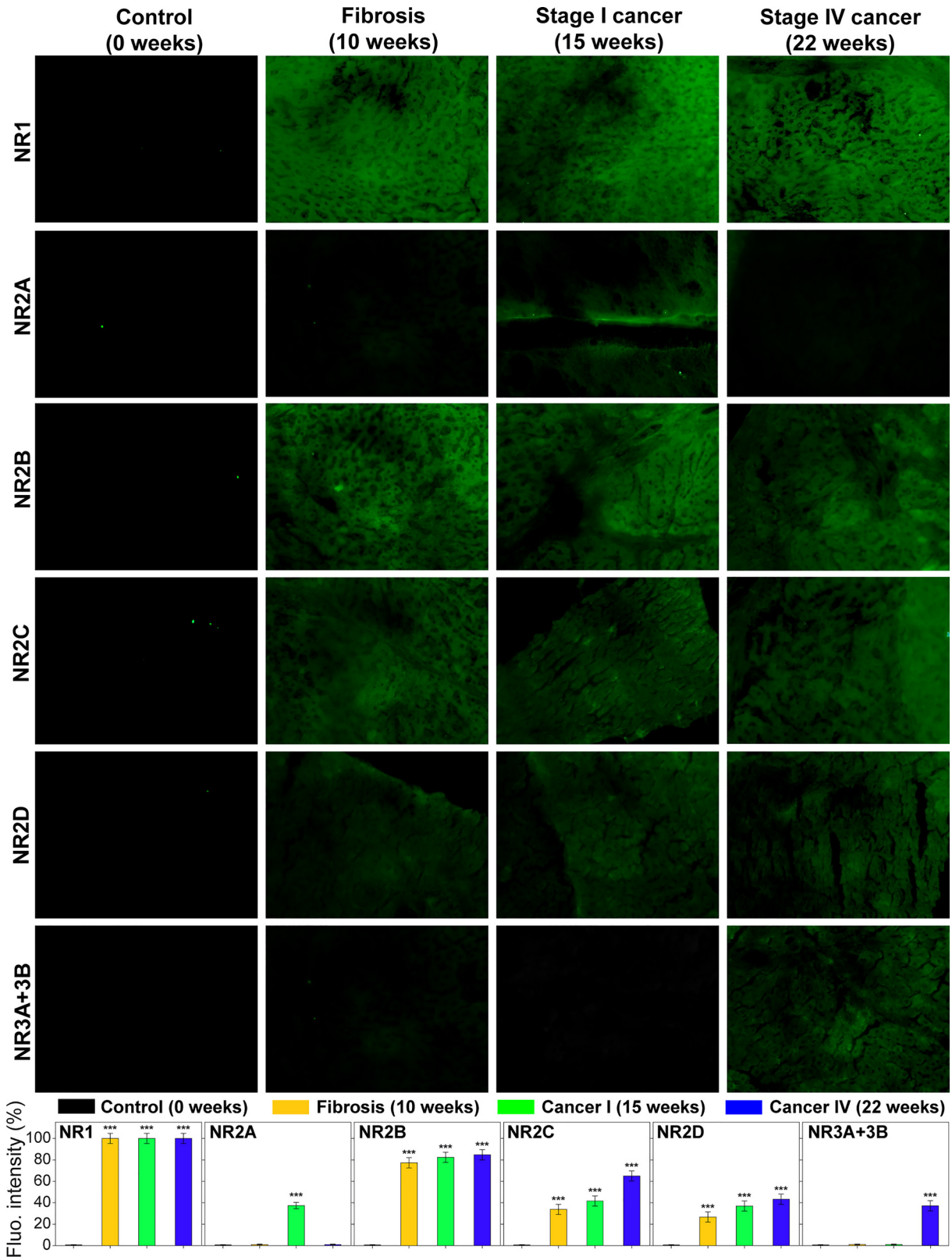

Figure 2. NR1 and NR2B-D subunits were detected via immunofluorescence in fibrotic and HCC livers and not in healthy controls. Fluorescence microscopy images of the expression of NMDAR NR1, NR2A/B/C/D, and NR3A/B subunits in rat liver tissues during the development from fibrosis toward HCC in comparison to control healthy liver are shown. The liver sections were immunofluorescently labeled with anti-NMDAR antibodies. The quantitation of the fluorescent signal from NMDAR subunits (obtained from the fluorescence images) is shown in the lower row. The data are presented as the mean ± SD (n = 10), ***$P < 0.001$ indicate a statistically significant difference (Student's t test). HCC, hepatocellular carcinoma; MNDAR, *N*-methyl-D-aspartate receptor.

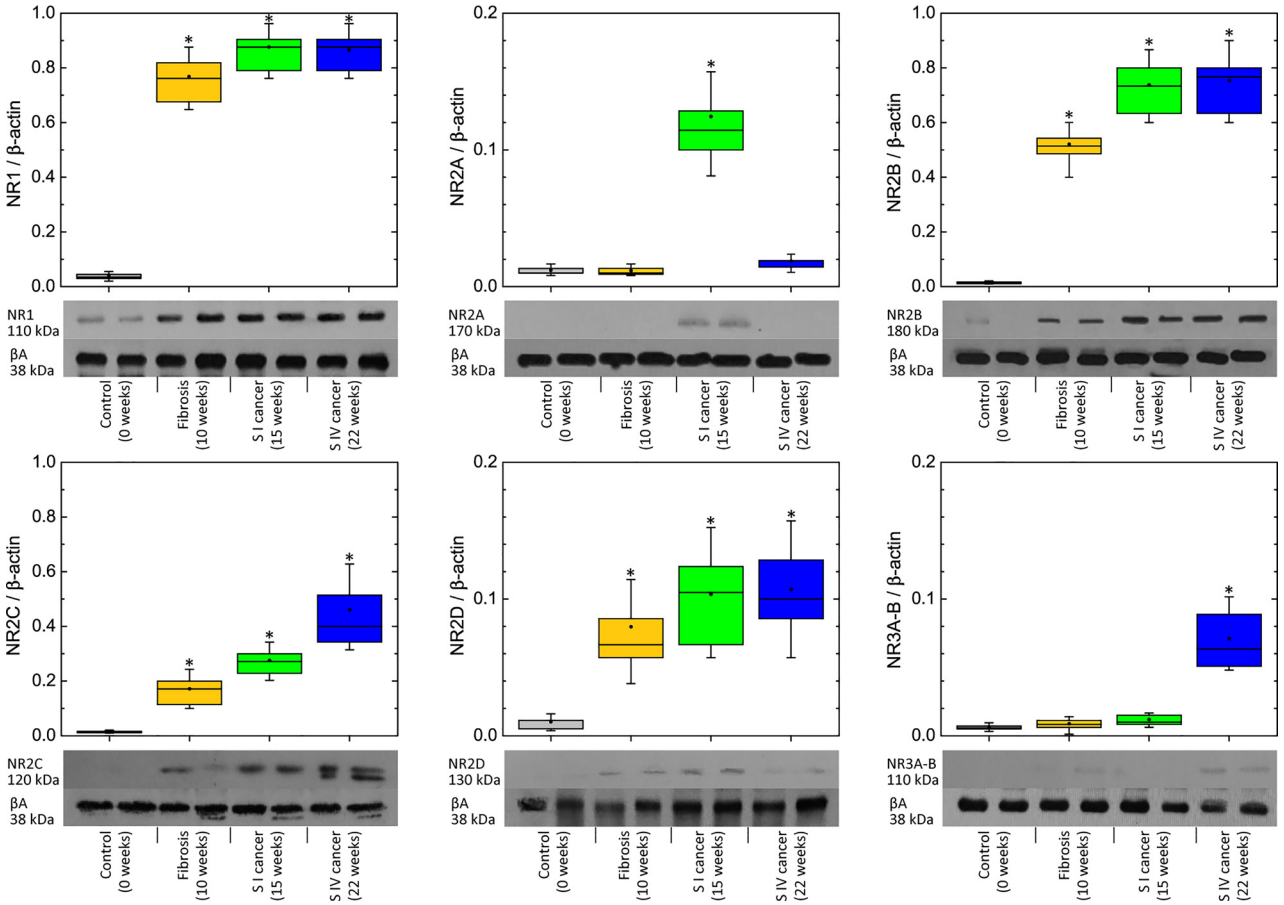

Figure 3. Box-and-whisker plots and photographs of Western blot gels representing expression of NR1 and NR2B–C subunits of the NMADR. Western blot analysis has been performed of the subcellular expression of NMDAR subunits in hepatocyte plasma membranes during the development of precancerous (fibrosis) and cancerous [HCC, stage (S) I and IV] livers in rats. 110–180 kDa is the size of NMDAR and 38 kDa is the size of β-actin (βA) protein detected in the hepatocyte plasma membranes fraction. For Western blot experiments, $n = 7$ in each group. Representative Western blot results for two animals per each group are depicted. *$P < 0.05$ indicates a statistically significant difference (Student's t test). HCC, hepatocellular carcinoma; MNDAR, *N*-methyl-D-aspartate receptor.

Decrease in DNA Methylation in *GRIN1*, *GRIN2A-B* Genes Is Observed Already at Fibrosis Stage of Liver Disease

Since the increase of gene expression can be mediated by changes in DNA methylation, we next focused on determination the methylation status of genes encoding NMDAR subunits. Direct bisulfite sequencing of the amplicons was performed to analyze the methylation level using forward primers. Therefore, the analysis included CpG sites from the 5'-end of CpG islands. Determination of the methylation sequence of CpG lanes by direct bisulfite sequencing began from the first methylated island in the promoter regions of genes.

Determination the methylation of studied genes was performed in each group of rats during fibrosis/HCC development. The CpG methylation status for *GRIN2A* and *GRIN2B* genes were determined in areas important for the transcription of these genes, previously identified in studies by Kiese et al. (47) and Parrish et al. (46). For the other two genes, *GRIN1* and *GRIN2C*, methylation was determined within CpG island sequences defined in the UCSC Genome Browser (Table 1). The *GRIN1* and *GRIN2C* changes in 19 and 30 sites of CpG islands, respectively, spanning the promoter region and the first exon of the gene (positions chr3:2,534,180–2,534,748 for *GRIN1* and chr10:103,816,343–103,816,962 for *GRIN2C*) were analyzed.

We have found a significant decrease in DNA methylation within the promoter region of *GRIN1* gene during tumor development for all CpG sites (Fig. 4*A*). The decrease in methylation of *GRIN1* gene by 43% was already observed at the stage of liver fibrosis, and during the subsequent HCC development (at I and IV cancer stages), the methylation was three times less than in control.

CpG methylation status of CpG-rich region in *GRIN2A* gene varied during liver disease development, in contrast to samples with *GRIN1* gene. Some islands showed a decrease, whereas others showed a slight increase in methylation levels (Fig. 4*B*); however, after 10, 15, and 22 wk, there were no significant changes in the methylation profile of the studied fragment.

In the analyzed region of *GRIN2B* gene CpG island, methylation of 20 CpG sites was determined (Fig. 4*C*). Already after 10 wk at fibrosis stage, demethylation of the entire CpG island was less by 32%. After 15 and 22 wk, the demethylation level of CpG sites remained lower by 19% and 31%, respectively, in comparison to control.

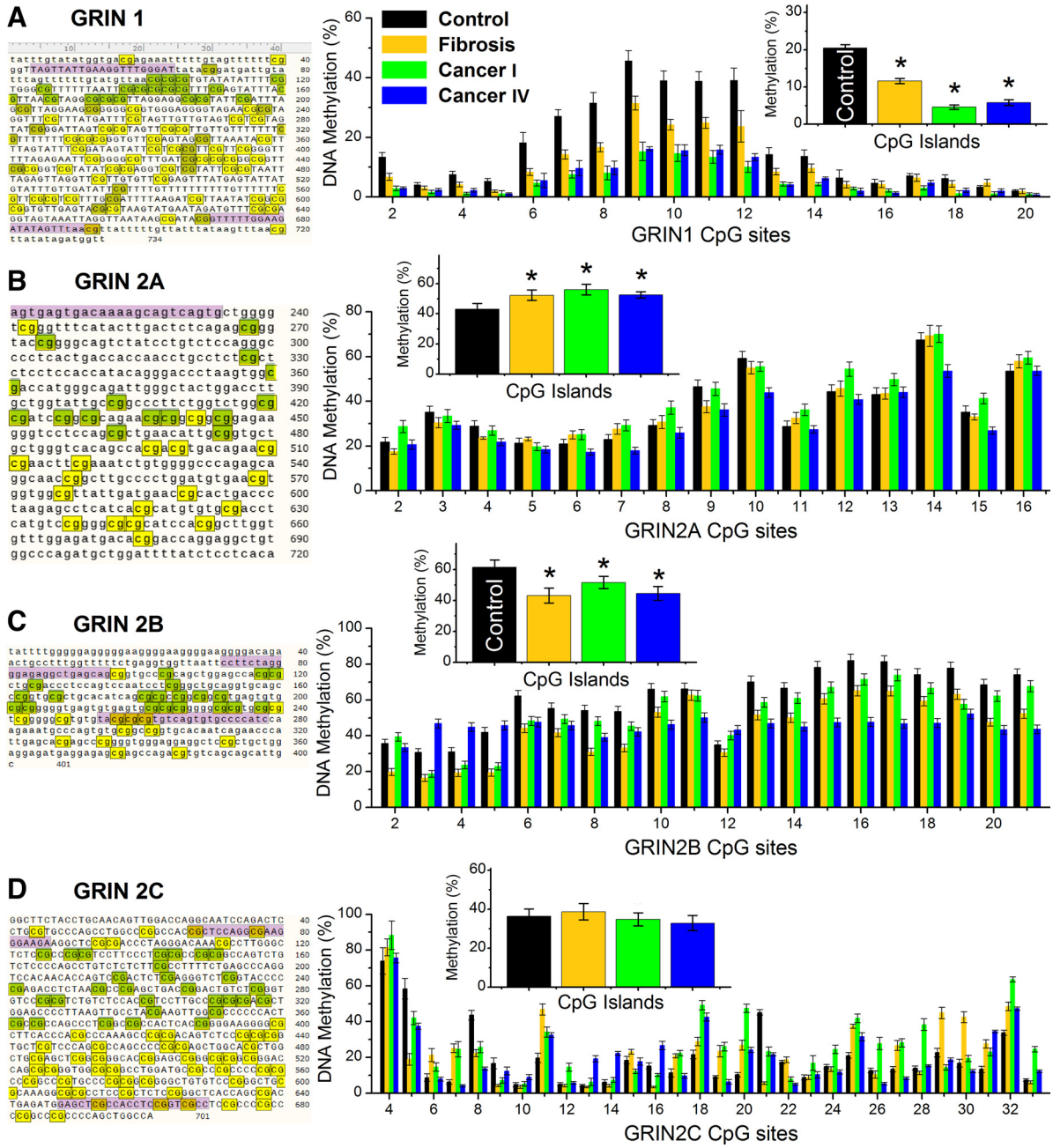

Figure 4. Decrease in DNA methylation observed in *GRIN1* and *GRIN2B* genes in fibrotic livers. DNA methylation levels for *GRIN1* (*A*), *GRIN2A* (*B*), *GRIN2B* (*C*), *GRIN2C* (*D*) gene in liver during fibrosis/HCC development were determined. The scheme shows all CpG islands (marked in green and yellow) in the promoter regions of genes, and CpG sites, methylation of which was investigated by direct bisulfite sequencing. Sequences of primers for amplification were marked in violet. The graphs show a change in DNA methylation levels of CpG islands and CpG sites in liver. Data were analyzed using Student's *t* test. The data are presented as the means ± SD, with $*P < 0.05$ compared with controls. (For *GRIN1* at 10 wk: $t = 3.16$, $*P < 0.05$, $n = 9$; at 15 wk: $t = 7.06$, $*P < 0.05$, $n = 7$; at 22 wk: $t = 6.01$, $*P < 0.05$, $n = 7$. For *GRIN2A* at 10 wk: $t = 0.08$, $*P > 0.05$, $n = 7$; at 15 wk: $t = 0.63$, $*P > 0.05$, $n = 7$; at 22 wk: $t = 1.16$, $*P > 0.05$, $n = 8$. For *GRIN2B* at 10 wk: $t = 3.29$, $*P < 0.05$, $n = 9$; at 15 wk: $t = 2.19$, $*P < 0.05$, $n = 9$; at 22 wk: $t = 2.71$, $*P < 0.05$, $n = 9$. For *GRIN2C* at 10 wk: $t = 2.05$, $*P = 0.057$, $n = 9$; at 15 wk: $t = 3.76$, $*P < 0.05$, $n = 8$; at 22 wk: $t = 1.11$, $*P > 0.05$, $n = 8$).

Results of DNA methylation analysis of CpG islands in the promoter region of *GRIN2C* gene were very complex. The methylation levels of 30 CpG studied sites, even in one position of DNA isolated from different animal at the same time point, were very different (Fig. 4*D*). On average, after 10 wk, differences in gene methylation were not observed, there was an increase (by 59%) in methylation after 15 wk of tumor development, then, after 22 wk, the methylation level of CpG sites returned to control values. A statistically significant decrease in methylation was determined in 5 CpG sites (5, 8, 9, 16, 21) after 10 wk and in 8 CpG sites (5, 8, 9, 15, 16, 21, 22, 29) after 15 wk. After 22 wk of tumor development, 7 of the 30 analyzed CpG sites had a reduced level of methylated cytosines (5, 8, 21, 22, 26, 27, 30) in tumor, compared with control samples (Fig. 4*D*). Other sites after 10, 15, and 22 wk have shown an increase in methylation levels.

Correlation Analysis

We further performed a correlation analysis comparing the methylated CpG islands in promoter region of genes and expression levels of NMDAR subunits (Fig. S5). GraphPad Prizm 7.0 software was used to perform the data analysis and the Pearson's correlation coefficient *r* was determined to confirm the relation between DNA methylation and the gene-expression level. The correlation between DNA methylation and gene expression at HCC development was determined to be negative for NR1 ($r = -0.9636$, $P = 0.0364$), NR2B ($r = -0.9501$, $P = 0.0498$), and NR2C ($r = -0.4377$, $P = 0.5623$) and positive for NR2A ($r = 0.6339$, $P = 0.3061$). As one can see, use of the analysis allowed us to find a significant correlation between an increase in the expression of NR1 and NR2B subunits, and a simultaneous decrease in methylation of CpG islands in the promoter of their genes. In contrast, the statistically significant correlation was not found for NR2C and NR2A subunits.

DISCUSSION

HCC is the most common primary liver cancer, accounting for more than 80% of all primary liver cancers (48). Carcinoma is characterized by a complex transformation etiology and requires a long-term treatment, even if the malignant process is detected at early stages. HCC is unsusceptible to radiotherapy, hepatic resection, and chemotherapy, and its postoperative recurrence is very common, which is the basic cause of the high mortality rate (49, 50). In this regard, liver cancer screening is the most urgent and important task that requires a reliable biomarker. The presence of a reliable biomarker in cancer patients in the pre- and post-therapeutic period is necessary to identify cell types that carry the risk of disease progression and subsequent post-therapeutic relapse (51). One of such biomarkers can be the NMDAR, which always appears in formed tumors (15–28), even in tissues where it is normally absent. Activation of NMDAR subunits expression is considered to be associated with tumor aggressiveness and poor prognosis, and overexpression of NR1 subunit has been shown to significantly correlate with tumor size, lymph node metastasis, and cancer stage (6, 33). NR2B subunit participates in regulation of various gene transcription, which is involved in cell cycle (31), and its overexpression is associated with the aggressiveness of certain cancer types (52). In support of this assumption, Gynther et al. (53) reported that interfering with lipid signaling pathways by inhibiting NMDARs could represent a new and promising treatment strategy for HCC. In this regard, the expression of NMDAR subunits in liver may serve as a biomarker for HCC progression. Accordingly, early diagnostics targeting NMDAR can be developed to achieve the reliable and safe therapy of liver cancer.

Using the model of liver HCC in rat, we have shown the NMDAR subunits appearing at the stage of liver fibrosis (10 wk), while these subunits are not observed in the liver tissue of healthy animals. During fibrosis period, fatty dystrophy of hepatocytes, eosinophilic cell alteration, and hepatocellular hypertrophy were observed, but neoplastic cell transformation was not recorded. NR1 and NR2B-C subunits expression was the most pronounced during this period, and recorded using immunohistochemistry (IHC), which also correlated with the results of Western blotting in any part of liver. Detection of these NMDAR subunits (NR1, NR2B, and NR2C) can serve as an important diagnostic factor, since this stage can be considered as a precancerous liver state. Formed at the stage of liver fibrosis, NR1, NR2B, and NR2C subunits are present throughout all liver cancer development.

The study of NMDAR subunits expression at 15 wk that corresponds to stage I cancer, in which the signs of macrolobular fibrosis, cirrhosis, neoplastic cell transformation, destruction of hepatocytes, and liver failure were observed, five NMDAR subunits were detected, NR1, NR2B, NR2C, and NR2D, in hepatocytes and NR2A in the bile duct walls. After 22 wk, when HCC has formed (stage IV cancer), six subunits were determined: NR1, NR2B, NR2C, NR2D, NR3A, and NR3B. The NR2A subunit expression was not recorded during this period.

Thus, it was found that NMDAR subunits are expressed at the stage of fibrosis, which can be considered as a precancerous stage of liver in HCC model. Although DEN is a traditional inducer for HCC model, other HCC models are further needed to elucidate the confounding effects. Experiments with other related animal models, such as transposon-based murine HCC (genotype: $p19^{Arf-/-}/NRAS^{G12V}$) and CCl_4-induced liver fibrosis in mice, allowed us to detect a pronounced NMDAR expression in the HCC-bearing animals. Importantly, the NR1 expression was not observed in CCl_4-induced liver fibrosis mouse model. CCl_4 injection in this model is known to cause hepatocyte damage, necrosis, inflammation, and fibrosis after 4 wk of administration (54). At the same time, fibrosis in this model does not lead to cancer development (54). Thus, the obtained results indicate that NMDAR expression occurs in more severe stages of fibrosis or precancerous liver disease, when cells undergo already neoplastic transformation that subsequently develops into liver cancer. The analysis of NMDAR expression has to be still verified, using human samples.

One of the reasons that significantly affects the transcriptional potential of individual genes is the methylation of cytosine nucleotides. Methylation instability has been shown in all neoplastic cells without exception (55). Such methylation usually occurs in cytosine-guanine dinucleotides, so-called "CpG" sites, which tend to accumulated in the promoter regions of gene. Methylation in CpG clusters long recognized as a major regulator of gene transcription (56). To the best of our knowledge, only few studies have investigated the methylation of NMDAR subunits, both in normal and pathological conditions (46, 47). Therefore, we carried out a deep study of the methylation degree encoding NMDAR subunits, the expression of which was activated during the fibrosis/HCC development.

Determination of NMDAR subunit methylation during fibrosis/HCC development, using bisulfite sequencing, showed a significant decrease in the *GRIN1* and *GRIN2B* gene methylation already at the stage of liver fibrosis (10 wk), which persisted at further tumor development. We observed a significant methylation decrease in 12 out of 19 CpG sites of *GRIN1* gene, and in 18 out of 20 CpG sites of *GRIN2B* gene. Demethylation of large amount of CpG islands in the promoter regions of *GRIN1* and *GRIN2B* genes at the stage of liver fibrosis can explain the expression of NR1 and NR2B subunits, which were recorded using IHC and Western blot methods.

A decreased methylation was not observed in *GRIN2A* genes. The obtained results are consistent with the Western blot data, where the NR2A subunit expression was weak or absent. NR2A expression was recorded using IHC (15 wk); however, this localization was detected only in bile ducts. For the Western blotting and determination of CpG islands, methylation samples were taken from liver fragments randomly, thus the bile ducts might not be taken into these samples, which affected the results.

The observed changes of the *GRIN2C* gene methylation profile were not significant. At the stage of liver fibrosis (10 wk), a decrease in methylation was noted at 5 from 30 analyzed sites, at 15 and 22 wk of fibrosis/HCC development 8 and 7 sites, respectively, had a reduced methylation level, all other sites had a tendency to increase methylation. Considering that increase in NR2C subunit expression was found using the IHC and Western blot methods at all stages of fibrosis/HCC development, we can suggest that either demethylation of these sites significantly affects the gene transcription, or along with epigenic changes, also genetic changes appear in the genes encoding the NR2C subunits during fibrosis/HCC development. The prevalence of somatic mutations of NMDAR subunits in malignant transformation has been confirmed in a number of studies (33, 34, 57).

A traditional view on the effects of DNA methylation on gene expression is that methylation of CpG sites in the promoter regions of genes corresponds to a decrease in gene expression. Using correlation analysis to determine the relationship between the methylation of CpG islands in the promoter regions of genes and NMDAR subunits expression, we found that the main reason for the increased NR1 and NR2B subunit expression is a decrease in CpG islands. Probably, the decrease in the methylation of genes encoding the NMDAR subunits can be considered as initial dynamic changes leading to an increase in the subunits expression.

Based on our experiments in rats and mice, we can consider NR1 and NR2B subunit expression at the stage of liver fibrosis as an early sign of cell malignancy, which occurs as a result of epigenetic changes in DNA during fibrosis/HCC development. Therefore, NMDAR attract interest for further study as a new biomarker in the early diagnosis of liver cancer. It remains to be elucidated whether the same NMDAR subunits are expressed in patients with fibrotic and cirrhotic livers of different etiologies, nonalcoholic fatty liver disease, and if NMDAR can be used as a universal marker in all precancerous liver diseases.

Conclusions

NMDAR expression during cell transformation process at the stages of HCC has been studied in rats and mice. NMDAR subunits were not detected in the liver tissue of healthy animals, but, in contrast, appeared at the stage of severe liver fibrosis and were increasingly expressed during the development of HCC. Furthermore, we have experimentally confirmed that NMDAR expression at the stage of liver fibrosis and following HCC progression is caused by demethylation of CpG islands in promoters of genes-encoding receptor subunits. This allows us to consider NMDAR expression as the early indicator of cancer cell transformation. We believe that the obtained results will pave the way for the use of NMDAR subunits as possible therapeutic targets and diagnostic biomarkers for the early detection of fibrotic livers or precancerous liver disease stage, which develops toward HCC in patients.

SUPPLEMENTAL DATA

All Supplemental material: https://doi.org/10.6084/m9.figshare.14014946.

GRANTS

Y.V.S., I.G., S.G., J.Q., T.Y.O. were supported in part by the National Natural Science Foundation of China Grants 61950410610, 61875135, 61525503, 61620106016, and 61835009; (Key) Project of Department of Education of Guangdong Province Grant 2016KCXTD007; and Shenzhen Basic Research Project Grant JCYJ20170818090620324. L.V.G. was supported by Ministry of Education and Science of Ukraine Grant 0118U000244. N.P. was supported by the German Academic Exchange Service (Deutscher Akademischer Austauschdienst, DAAD) in the scope of the Doctoral Program in Germany 2019/2021 under grant (Project-ID 91736778). T.Y. was supported by the German Research Foundation (DFG, Grant YE151/2-1, AOBJ: 618426 and Gilead Sciences International Research Scholars Program in Liver Disease.

DISCLOSURES

No conflicts of interest, financial or otherwise, are declared by the authors.

AUTHOR CONTRIBUTIONS

Y.V.S. and L.V.G. conceived and designed research; Y.V.S., I.G., N.V.D., H.M.K., N.P., I.S., L.I.S., Y.S., and T.Y. performed experiments; Y.V.S., I.G., and S.G. analyzed data; Y.V.S. and I.G. interpreted results of experiments; Y.V.S., I.G., and S.G. prepared figures; Y.V.S., I.G., and S.G. drafted manuscript; S.G., T.Y., J.Q., and T.Y.O. edited and revised manuscript; L.V.G., L.I.O., J.Q., and T.Y.O. approved final version of manuscript.

REFERENCES

1. **European Association for the Study of the Liver**. EASL clinical practice guidelines: management of hepatocellular carcinoma. *J Hepatol* 69: P182–P236, 2018. doi:10.1016/j.jhep.2018.03.019.
2. **Jackson PE**, **Groopman JD.** Aflatoxin and liver cancer. *Baillieres Best Pract Res Clin Gastroenterol* 13: 545–555, 1999. doi:10.1053/bega.1999.0047.
3. **Ahn SM**, **Jang SJ**, **Shim JH**, **Kim D**, **Hong SM**, **Sung CO**, **Baek D**, **Haq F**, **Ansari AA**, **Lee SY**, **Chun SM**, **Choi S**, **Choi HJ**, **Kim J**, **Kim S**, **Hwang S**, **Lee YJ**, **Lee JE**, **Jung WR**, **Jang HY**, **Yang E**, **Sung WK**, **Lee NP**, **Mao M**, **Lee C**, **Zucman-Rossi J**, **Yu E**, **Lee HC**, **Kong G.** Genomic portrait of resectable hepatocellular carcinomas: implications of RB1 and FGF19 aberrations for patient stratification. *Hepatology* 60: 1972–1982, 2014. doi:10.1002/hep.27198.
4. **Mirshahi F**, **Aqbi HF**, **Cresswell K**, **Saneshaw M**, **Coleman C**, **Jacobs T**, **Idowu MO**, **Dozmorov M**, **Sanyal AJ**, **Manjili MH.** Longitudinal studies can identify distinct inflammatory cytokines associated with the inhibition or progression of liver cancer. *Liver Int* 40: 468–472, 2020. doi:10.1111/liv.14323.
5. **Yu LJ**, **Wall BA**, **Wangari-Talbot J**, **Chen S.** Metabotropic glutamate receptors in cancer. *Neuropharmacology* 115: 193–202, 2017. doi:10.1016/j.neuropharm.2016.02.011.
6. **Stepulak A**, **Rola R**, **Polberg K**, **Ikonomidou C.** Glutamate and its receptors in cancer. *J Neural Transm (Vienna)* 121: 933–944, 2014. doi:10.1007/s00702-014-1182-6.

7. **Kew JNC**, **Kemp JA.** Ionotropic and metabotropic glutamate receptor structure and pharmacology. *Psychopharmacology (Berl)* 179: 4–29, 2005. [Erratum in *Psychopharmacology (Berl)* 182: 320, 2005] doi:10.1007/s00213-005-2200-z.
8. **Traynelis SF**, **Wollmuth LP**, **McBain CJ**, **Menniti FS**, **Vance KM**, **Ogden KK**, **Hansen KB**, **Yuan H**, **Myers SJ**, **Dingledine R.** Glutamate receptor ion channels: structure, regulation, and function. *Pharmacol Rev* 62: 405–496, 2010. [Erratum in *Pharmacol Rev* 66: 1141, 2014]. doi:10.1124/pr.109.002451.
9. **Sequerra EB**, **Goyal R**, **Castro PA**, **Levin JB**, **Borodinsky LN.** NMDA Receptor signaling is important for neural tube formation and for preventing antiepileptic drug-induced neural tube defects. *J Neurosci* 38: 4762–4773, 2018. [Erratum in *J Neurosci* 38: 10399, 2018] doi:10.1523/JNEUROSCI.2634-17.2018.
10. **Tamura H**, **Suzuki M**, **Moriya Y**, **Hoshino H**, **Okamoto T**, **Yoshida S**, **Yoshino I.** Aberrant methylation of N-methyl-D-aspartate receptor type 2B (NMDAR2B) in non-small cell carcinoma. *BMC Cancer* 11: 220–228, 2011. doi:10.1186/1471-2407-11-220.
11. **Ganor Y**, **Levite M.** Glutamate in the immune system: Glutamate receptors in immune cells, potent effects, endogenous production and involvement in disease. In: *Nerve-Driven Immunity Neurotransmitters and Neuropeptides in the Immune System*, edited by Levite M. Vienna: Springer-Verlag, 2012, p. 121–161.
12. **Seo JH**, **Fox JG**, **Peek RM Jr**, **Hagen SJ.** N-methyl D-aspartate channels link ammonia and epithelial cell death mechanisms in Helicobacter pylori infection. *Gastroenterology* 141: 2064–2075, 2011. doi:10.1053/j.gastro.2011.08.048.
13. **Golovynska I**, **Beregova TV**, **Falalyeyeva TM**, **Stepanova LI**, **Golovynskyi S**, **Qu J**, **Ohulchanskyy TY.** Peripheral N-methyl-D-aspartate receptor localization and role in gastric acid secretion regulation: immunofluorescence and pharmacological studies. *Sci Rep* 8: 7445–7456, 2018. doi:10.1038/s41598-018-25753-6.
14. **Yue Y**, **Luo Z**, **Liao Z**, **Zhang L**, **Liu S**, **Wang M**, **Zhao F**, **Cao C**, **Ding Y**, **Yue S.** Excessive activation of NMDA receptor inhibits the protective effect of endogenous bone marrow mesenchymal stem cells on promoting alveolarization in bronchopulmonary dysplasia. *Am J Physiol Cell Physiol* 316: C815–C827, 2019. doi:10.1152/ajpcell.00392.2018.
15. **Duan W**, **Hu J**, **Liu Y.** Ketamine inhibits colorectal cancer cells malignant potential via blockage of NMDA receptor. *Exp Mol Pathol* 107: 171–178, 2019. doi:10.1016/j.yexmp.2019.02.004.
16. **Abdul M**, **Hoosein N.** N-methyl-D-aspartate receptor in human prostate cancer. *J Membr Biol* 205: 125–128, 2005. doi:10.1007/s00232-005-0777-0.
17. **Shin S-S**, **Namkoong J**, **Wall BA**, **Gleason R**, **Lee HJ**, **Chen S.** Oncogenic activities of metabotropic glutamate receptor 1 (Grm1) in melanocyte transformation. *Pigment Cell Melanoma Res* 21: 368–378, 2008. doi:10.1111/j.1755-148X.2008.00452.x.
18. **Gorska-Ponikowska M**, **Perricone U**, **Kuban-Jankowska A**, **Lo Bosco G**, **Barone G.** 2-methoxyestradiol impacts on amino acids-mediated metabolic reprogramming in osteosarcoma cells by its interaction with NMDA receptor. *J Cell Physiol* 232: 3030–3049, 2017. doi:10.1002/jcp.25888.
19. **Watanabe K**, **Kanno T**, **Oshima T**, **Miwa H**, **Tashiro C**, **Nishizaki T.** The NMDA receptor NR2A subunit regulates proliferation of MKN45 human gastric cancer cells. *Biochem Biophys Res Commun* 367: 487–490, 2008. doi:10.1016/j.bbrc.2007.12.167.
20. **Kang M**, **Cho JH**, **Koo JK**, **Noh SU**, **Kim M-Y**, **Kang H**, **Oh ST**, **Kim HO**, **Park YM.** The expression of NMDA receptor 1 correlates with clinicopathological parameters in cutaneous squamous cell carcinoma. *Ann Dermatol* 21: 382–388, 2009. doi:10.5021/ad.2009.21.4.382.
21. **Ganor Y**, **Grinberg I**, **Reis A**, **Cooper I**, **Goldstein RS**, **Levite M.** Human T-leukemia and T-lymphoma express glutamate receptor AMPA GluR3, and the neurotransmitter glutamate elevates the cancer-related matrix-metalloproteinases inducer CD147/EMMPRIN, MMP-9 secretion and engraftment of T-leukemia in vivo. *Leuk Lymphoma* 50: 985–997, 2009. doi:10.1080/10428190902878448.
22. **Stepulak A**, **Luksch H**, **Gebhardt C**, **Uckermann O**, **Marzahn J**, **Sifringer M**, **Rzeski W**, **Staufner C**, **Brocke KS**, **Turski L**, **Ikonomidou C.** Expression of glutamate receptor subunits in human cancers. *Histochem Cell Biol* 132: 435–445, 2009. doi:10.1007/s00418-009-0613-1.
23. **William G. North W.** NMDA receptors are expressed by small-cell lung cancer and are potential targets for effective treatment. *Clin Pharmacol* 2: 31–40, 2010. doi:10.2147/CPAA.S6262.
24. **North WG**, **Gao G**, **Memoli VA**, **Pang RH**, **Lynch L.** Breast cancer expresses functional NMDA receptors. *Breast Cancer Res Treat* 122: 307–314, 2010. doi:10.1007/s10549-009-0556-1.
25. **Herner A**, **Sauliunaite D**, **Michalski CW**, **Erkan M**, **Oliveira TD**, **Abiatari I**, **Kong B**, **Esposito I**, **Friess H**, **Kleeff J.** Glutamate increases pancreatic cancer cell invasion and migration via AMPA receptor activation and Kras-MAPK signaling. *Int J Cancer* 129: 2349–2359, 2011. doi:10.1002/ijc.25898.
26. **Stepulak A**, **Luksch H**, **Uckermann O**, **Sifringer M**, **Rzeski W**, **Polberg K**, **Kupisz K**, **Klatka J**, **Kielbus M**, **Grabarska A**, **Marzahn J**, **Turski L**, **Ikonomidou C.** Glutamate receptors in laryngeal cancer cells. *Anticancer Res* 31: 565–574, 2011.
27. **Yamaguchi F**, **Hirata Y**, **Akram H**, **Kamitori K**, **Dong Y**, **Sui L**, **Tokuda M.** FOXO/TXNIP pathway is involved in the suppression of hepatocellular carcinoma growth by glutamate antagonist MK-801. *BMC Cancer* 13: 468–479, 2013. doi:10.1186/1471-2407-13-468.
28. **Choi CH**, **Choi JJ**, **Park YA**, **Lee YY**, **Song SY**, **Sung CO**, **Song T**, **Kim MK**, **Kim TJ**, **Lee JW**, **Kim HJ**, **Bae DS**, **Kim BG.** Identification of differentially expressed genes according to chemosensitivity in advanced ovarian serous adenocarcinomas: Expression of GRIA2 predicts better survival. *Br J Cancer* 107: 91–99, 2012. doi:10.1038/bjc.2012.217.
29. **Luksch H**, **Uckermann O**, **Stepulak A**, **Hendruschk S**, **Marzahn J**, **Bastian S**, **Staufner C**, **Temme A**, **Ikonomidou C.** Silencing of selected glutamate receptor subunits modulates cancer growth. *Anticancer Res* 31: 3181–3192, 2011.
30. **Golovynska I**, **Golovynskyi SL**, **Stepanov YV**, **Garmanchuk LV**, **Stepanova LI**, **Qu J**, **Ohulchanskyy TY.** Red and near-infrared light induces intracellular Ca^{2+} flux via the activation of glutamate N-methyl-D-aspartate receptors. *J Cell Physiol* 234: 15989–16002, 2019. doi:10.1002/jcp.28257.
31. **Deutsch SI**, **Tang AH**, **Burket JA**, **Benson AD.** NMDA receptors on the surface of cancer cells: target for chemotherapy? *Biomed Pharmacother* 68: 493–496, 2014. doi:10.1016/j.biopha.2014.03.012.
32. **Pópulo H**, **Lopes JM**, **Soares P.** The mTOR signalling pathway in human cancer. *Int J Mol Sci* 13: 1886–1918, 2012. doi:10.3390/ijms13021886.
33. **Wei X**, **Walia V**, **Lin JC**, **Teer JK**, **Prickett TD**, **Gartner J**, **Davis S**; **NISC Comparative Sequencing Program**; **Stemke-Hale K**, **Davies MA**, **Gershenwald JE**, **Robinson W**, **Robinson S**, **Rosenberg SA**, **Samuels Y.** Exome sequencing identifies GRIN2A as frequently mutated in melanoma. *Nat Genet* 43: 442–446, 2011. doi:10.1038/ng.810.
34. **Prickett TD**, **Zerlanko BJ**, **Hill VK**, **Gartner JJ**, **Qutob N**, **Jiang J**, **Simaan M**, **Wunderlich J**, **Gutkind JS**, **Rosenberg SA**, **Samuels Y.** Somatic mutation of GRIN2A in malignant melanoma results in loss of tumor suppressor activity via aberrant NMDAR complex formation. *J Invest Dermatol* 134: 2390–2398, 2014. doi:10.1038/jid.2014.190.
35. **Liu J-W**, **Kim MS**, **Nagpal J**, **Yamashita K**, **Poeta L**, **Chang X**, **Lee J**, **Park HL**, **Jeronimo C**, **Westra WH**, **Mori M**, **Moon C**, **Trink B**, **Sidransky D.** Quantitative hypermethylation of NMDAR2B in human gastric cancer. *Int J Cancer* 121: 1994–2000, 2007. doi:10.1002/ijc.22934.
36. **Park SY**, **Kwon HJ**, **Lee HE**, **Ryu HS**, **Kim SW**, **Kim JH**, **Kim IA**, **Jung N**, **Cho NY**, **Kang GH.** Promoter CpG island hypermethylation during breast cancer progression. *Virchows Arch* 458: 73–84, 2011. doi:10.1007/s00428-010-1013-6.
37. **Kim MS**, **Yamashita K**, **Baek JH**, **Park HL**, **Carvalho AL**, **Osada M**, **Hoque MO**, **Upadhyay S**, **Mori M**, **Moon C**, **Sidransky D.** N-methyl-D-aspartate receptor type 2B is epigenetically inactivated and exhibits tumor-suppressive activity in human esophageal cancer. *Cancer Res* 66: 3409–3418, 2006. doi:10.1158/0008-5472.CAN-05-1608.
38. **Liu XQ**, **Hu XJ**, **Xu HX**, **Zeng XY.** Xiaochaihu Decoction attenuates the vicious circle between the oxidative stress and the ALP inactivation through LPS-catecholamines interactions in gut, liver and brain during CCl4 + ethanol-induced mouse HCC. *BMC Complem Altern M* 13: 375–385, 2013. doi:10.1186/1472-6882-13-375.
39. **Song G**, **Pacher M**, **Balakrishnan A**, **Yuan Q**, **Tsay H-C**, **Yang D**, **Reetz J**, **Brandes S**, **Dai Z**, **Pützer BM**, **Araúzo-Bravo MJ**, **Steinemann D**, **Luedde T**, **Schwabe RF**, **Manns MP**, **Schöler HR**,

Schambach A, **Cantz T**, **Ott M**, **Sharma AD.** Direct reprogramming of hepatic myofibroblasts into hepatocytes in vivo attenuates liver fibrosis. *Cell Stem Cell* 18: 797–808, 2016. doi:10.1016/j.stem.2016.01.010.

40. **Wuestefeld T**, **Pesic M**, **Rudalska R**, **Dauch D**, **Longerich T**, **Kang T-W**, **Yevsa T**, **Heinzmann F**, **Hoenicke L**, **Hohmeyer A**, **Potapova A**, **Rittelmeier I**, **Jarek M**, **Geffers R**, **Scharfe M**, **Klawonn F**, **Schirmacher P**, **Malek NP**, **Ott M**, **Nordheim A**, **Vogel A**, **Manns MP**, **Zender L.** A direct in vivo RNAi screen identifies MKK4 as a key regulator of liver regeneration. *Cell* 153: 389–401, 2013. doi:10.1016/j.cell.2013.03.026.
41. **Kamijo T**, **Zindy F**, **Roussel MF**, **Quelle DE**, **Downing JR**, **Ashmun RA**, **Grosveld G**, **Sherr CJ.** Tumor suppression at the mouse INK4a locus mediated by the alternative reading frame product p19 ARF. *Cell* 91: 649–659, 1997. doi:10.1016/S0092-8674(00)80452-3.
42. **Dauch D**, **Rudalska R**, **Cossa G**, **Nault J-C**, **Kang T-W**, **Wuestefeld T**, **Hohmeyer A**, **Imbeaud S**, **Yevsa T**, **Hoenicke L**, **Pantsar T**, **Bozko P**, **Malek NP**, **Longerich T**, **Laufer S**, **Poso A**, **Zucman-Rossi J**, **Eilers M**, **Zender LA.** MYC–aurora kinase A protein complex represents an actionable drug target in p53-altered liver cancer. *Nat Med* 22: 744–753, 2016. doi:10.1038/nm.4107.
43. **Kang T-W**, **Yevsa T**, **Woller N**, **Hoenicke L**, **Wuestefeld T**, **Dauch D**, **Hohmeyer A**, **Gereke M**, **Rudalska R**, **Potapova A**, **Iken M**, **Vucur M**, **Weiss S**, **Heikenwalder M**, **Khan S**, **Gil J**, **Bruder D**, **Manns M**, **Schirmacher P**, **Tacke F**, **Ott M**, **Luedde T**, **Longerich T**, **Kubicka S**, **Zender L.** Senescence surveillance of pre-malignant hepatocytes limits liver cancer development. *Nature* 479: 547–551, 2011. doi:10.1038/nature10599.
44. **Petriv N**, **Neubert L**, **Vatashchuk M**, **Timrott K**, **Suo H**, **Hochnadel I**, **Huber R**, **Petzold C**, **Hrushchenko A**, **Yatsenko AS**, **Shcherbata HR**, **Wedemeyer H**, **Lichtinghagen R**, **Falfushynska H**, **Lushchak V**, **Manns MP**, **Bantel H**, **Semchyshyn H**, **Yevsa T.** Increase of α-dicarbonyls in liver and receptor for advanced glycation end products on immune cells are linked to nonalcoholic fatty liver disease and liver cancer. *Oncoimmunology* 10: 1874159, 2021. doi:10.1080/2162402X.2021.1874159.
45. **Parrish RR**, **Day JJ**, **Lubin FD.** Direct bisulfite sequencing for examination of DNA methylation with gene and nucleotide resolution from brain tissues. *Curr Protoc Neurosci* 60: 7.24.1–7.24.12, 2012. doi:10.1002/0471142301.ns0724s60.
46. **Parrish RR**, **Albertson AJ**, **Buckingham SC**, **Hablitz JJ**, **Mascia KL**, **Haselden DW**, **Lubin FD.** Status epilepticus triggers early and late alterations in brain-derived neurotrophic factor and NMDA glutamate receptor Grin2b DNA methylation levels in the hippocampus. *Neuroscience* 248: 602–619, 2013. doi:10.1016/j.neuroscience.2013.06.029.
47. **Kiese K**, **Jablonski J**, **Hackenbracht J**, **Wrosch JK**, **Groemer TW**, **Kornhuber J**, **Blümcke I**, **Kobow K.** Epigenetic control of epilepsy target genes contributes to a cellular memory of epileptogenesis in cultured rat hippocampal neurons. *Acta Neuropathol Commun* 5: 79–93, 2017. doi:10.1186/s40478-017-0485-x.
48. **Yang JD**, **Hainaut P**, **Gores GJ**, **Amadou A**, **Plymoth A**, **Roberts LR.** A global view of hepatocellular carcinoma: trends, risk, prevention and management. *Nat Rev Gastroenterol Hepatol* 16: 589–604, 2019. doi:10.1038/s41575-019-0186-y.
49. **Zhang Y**, **Li D**, **Feng F**, **An L**, **Hui F**, **Dang D**, **Zhao Q.** Progressive and prognosis value of notch receptors and ligands in hepatocellular carcinoma: a systematic review and meta-analysis. *Sci Rep* 7: 14809, 2017. doi:10.1038/s41598-017-14897-6.
50. **Bak-Fredslund KP**, **Keiding S**, **Villadsen GE**, **Kramer S**, **Schlander S**, **Sørensen M.** [^{18}F]-Fluoro-2-deoxy-D-galactose positron emission tomography/computed tomography as complementary imaging tool in patients with hepatocellular carcinoma. *Liver Int* 40: 447–455, 2020. doi:10.1111/liv.14293.
51. **Walcher L**, **Kistenmacher A-K**, **Suo H**, **Kitte R**, **Dluczek S**, **Strauß A**, **Blaudszun AR**, **Yevsa T**, **Fricke S**, **Kossatz-Boehlert U.** Cancer stem cells—origins and biomarkers: perspectives for targeted personalized therapies. *Front Immunol* 11: 1280, 2020. doi:10.3389/fimmu.2020.01280.
52. **Li L**, **Hanahan D.** Hijacking the neuronal NMDAR signaling circuit to promote tumor growth and invasion. *Cell* 153: 86–100, 2013. doi:10.1016/j.cell.2013.02.051.
53. **Gynther M**, **Proietti Silvestri I**, **Hansen JC**, **Hansen KB**, **Malm T**, **Ishchenko Y**, **Larsen Y**, **Han L**, **Kayser S**, **Auriola S**, **Petsalo A**, **Nielsen B**, **Pickering DS**, **Bunch L.** Augmentation of anticancer drug efficacy in murine hepatocellular carcinoma cells by a peripherally acting competitive N-Methyl-d-aspartate (NMDA) receptor antagonist. *J Med Chem* 60: 9885–9904, 2017. doi:10.1021/acs.jmedchem.7b01624.
54. **Scholten D**, **Trebicka J**, **Liedtke C**, **Weiskirchen R.** The carbon tetrachloride model in mice. *Lab Anim* 49: 4–11, 2015. doi:10.1177/0023677215571192.
55. **Scala G**, **Federico A**, **Palumbo D**, **Cocozza S**, **Greco D.** DNA sequence context as a marker of CpG methylation instability in normal and cancer tissues. *Sci Rep* 10: 1721–1732, 2020. doi:10.1038/s41598-020-58331-w.
56. **Jaenisch R**, **Bird A.** Epigenetic regulation of gene expression: how the genome integrates intrinsic and environmental signals. *Nat Genet* 33: 245–254, 2003. doi:10.1038/ng1089.
57. **Endele S**, **Rosenberger G**, **Geider K**, **Popp B**, **Tamer C**, **Stefanova I**, **Milh M**, **Kortüm F**, **Fritsch A**, **Pientka FK**, **Hellenbroich Y**, **Kalscheuer VM**, **Kohlhase J**, **Moog U**, **Rappold G**, **Rauch A**, **Ropers HH**, **von Spiczak S**, **Tönnies H**, **Villeneuve N**, **Villard L**, **Zabel B**, **Zenker M**, **Laube B**, **Reis A**, **Wieczorek D**, **Van Maldergem L**, **Kutsche K.** Mutations in GRIN2A and GRIN2B encoding regulatory subunits of NMDA receptors cause variable neurodevelopmental phenotypes. *Nat Genet* 42: 1021–1026, 2010. doi:10.1038/ng.677.